



A path integral approach to the Hodgkin–Huxley model



Roman Baravalle^{a,b}, Osvaldo A. Rosso^{c,d,e}, Fernando Montani^{a,b,*}

^a IFLYSIB, CONICET & Universidad Nacional de La Plata, Calle 59-789, (1900) La Plata, Argentina

^b Departamento de Física, Facultad de Ciencias Exactas, Universidad Nacional de La Plata, Calle 49 y 115. C.C. 67, (1900) La Plata, Argentina

^c Departamento de Informática en Salud, Hospital Italiano de Buenos Aires & CONICET, C1199ABB Ciudad Autónoma de Buenos Aires, Argentina

^d Instituto de Física, Universidade Federal de Alagoas (UFAL), 57072-900 Maceió, Brazil

^e Complex Systems Group, Facultad de Ingeniería y Ciencias Aplicadas, Universidad de los Andes, 12455 Santiago, Chile

HIGHLIGHTS

- We need to develop stochastic models describing the neuronal dynamics.
- Stochastic systems can be expressed in terms of path integrals.
- Noise processes are induced by the neural network/feedforward correlations.
- We obtain path integral solutions driven by a non-Gaussian colored noise q .
- Allows us to investigate the underlying dynamics of the neural system.

ARTICLE INFO

Article history:

Received 6 April 2017

Received in revised form 28 May 2017

Available online 24 June 2017

Keywords:

Neuronal model

Path integrals

Stochastic processes

Spiking output

Neural coding

ABSTRACT

To understand how single neurons process sensory information, it is necessary to develop suitable stochastic models to describe the response variability of the recorded spike trains. Spikes in a given neuron are produced by the synergistic action of sodium and potassium of the voltage-dependent channels that open or close the gates. Hodgkin and Huxley (HH) equations describe the ionic mechanisms underlying the initiation and propagation of action potentials, through a set of nonlinear ordinary differential equations that approximate the electrical characteristics of the excitable cell. Path integral provides an adequate approach to compute quantities such as transition probabilities, and any stochastic system can be expressed in terms of this methodology. We use the technique of path integrals to determine the analytical solution driven by a non-Gaussian colored noise when considering the HH equations as a stochastic system. The different neuronal dynamics are investigated by estimating the path integral solutions driven by a non-Gaussian colored noise q . More specifically we take into account the correlational structures of the complex neuronal signals not just by estimating the transition probability associated to the Gaussian approach of the stochastic HH equations, but instead considering much more subtle processes accounting for the non-Gaussian noise that could be induced by the surrounding neural network and by feedforward correlations. This allows us to investigate the underlying dynamics of the neural system when different scenarios of noise correlations are considered.

© 2017 Published by Elsevier B.V.

* Corresponding author at: IFLYSIB, CONICET & Universidad Nacional de La Plata, Calle 59-789, (1900) La Plata, Argentina
E-mail address: fmontani@gmail.com (F. Montani).

1. Introduction

To understand how information is transported in cerebral cortex we need to investigate first the input and output characteristics of a given neuron. The membrane potential is the difference in electric potential between the interior and exterior of the cell, where the surrounding extracellular fluid is located. The resting potential tells us what happens when a neuron is at rest, at a voltage of -70 mV. The voltage in the membrane of a neuron depends on currents from a diverse collection of ion channels, many of which have nonlinear voltage-dependent dynamics [1–5]. General forms for the dynamics of many of the major families of ion channels have been characterized [2,6], but the kinetic parameters vary according to the neuron where the ion channels are located. A spike occurs when a neuron sends information down an axon, away from the cell body as an explosion of electrical activity that is created by a depolarizing current. At the single neuron level neurophysiology recordings allow to accurately measure the membrane potential showing that neurons exhibit rich dynamical behaviors, including rhythmic bursting and patterned sequence generation [5,7–9]. These dynamics derive from the intrinsic properties of individual neurons and from the connections among them within the network. That is neurons, under the current framework, behave similarly to nonlinear oscillators [10].

The path integral method provides us with the means to estimate unmeasured states and parameters conditioned on measurements of some subset of the variables. Moreover, the method is exact, as an exact statement of the information transfer at each measurement comes from an identity on conditional probabilities [11,12]. It has the advantage of combining the local uncertainty in state to state transitions with the global trajectory of the system. This provides an integral representation of the linear partial differential equation for the conditional probability distribution. As such delivers a global view of the solution to the underlying stochastic physical problem and permits going beyond the local view of other methodologies [11–15]. The path integral also takes into account the paths of a stochastic system through its state space as they are influenced by observations. Thus, we have to focus first on the formulation of the questions one wants to answer using the path integral formulation to then developing a methodology to perform the integrals that answer those questions avoiding the limitations of other methods [12]. Stochastic differential equations can be used to model the phenomena of the neuronal firing [16]. Importantly, any stochastic and even deterministic system can be expressed in terms of path integrals that provide a convenient tool to compute quantities such as transition probabilities [11–16].

HH equations allows us to explain how action potentials are generated through the electrical excitability of neuronal membranes [17–21]. The path integral methodology can provide us an alternative approach to determinate the analytical solution of the membrane potential when considering the stochastic HH equations. In this paper we consider the path integral solution driven by a non-Gaussian colored noise of the HH equations as a stochastic system. We develop a path integral formulation for characterizing the different states of a neuron as non-linear dynamical system considering colored noise that could account for the possible effects of the surrounding background activity, correlated activity, feedforward correlations, and the ephaptic coupling [22], as they might alter the functioning of individual neurons and neural assemblies under different physiological conditions. In order to do it so we use a variational method to minimize the action of the path integral formulation [11,12,23]. We apply the methodology of path integrals developed by Wio et al. considering a colored noise within the q -Gaussian formalism [11–13]. More specifically, we investigate the solutions of HH equation as a particular case of the Fokker–Planck equation driven by a non-Gaussian colored noise q that is better suited to be investigated within the path integral approach. We analyze the causality entropy–complexity plane $H \times C$ and causal Fisher information versus statistical complexity/Shannon entropy, $F \times C$ and $F \times H$, considering the solution of the path integral formulation driven by different levels of noise q . This allows us to investigate the underlying dynamics of the neural system, quantifying the degree of correlations in the neural responses.

2. Methodology

2.1. Model

Let us consider first the biophysical model for the membrane potential V of a section of a spatially homogeneous neuron, the HH model reads as [17]:

$$C_m \frac{dV}{dt} = -I_{Na} - I_K - I_M - g_L(V - E_L) - \frac{1}{A} I_{syn} \quad (1)$$

where

$$\begin{aligned} I_{Na} &= \bar{g}_{Na} P_{Na}(V, t)(V - E_{Na}), \\ I_K &= \bar{g}_K P_K(V, t)(V - E_K), \\ I_M &= \bar{g}_M P_M(V, t)(V - E_M). \end{aligned}$$

Here C_m is the membrane capacitance, g_X is the maximal conductance of channels of type X , P_X is the probability that a channel of type X is open, E_X is the reversal potential for channel type X and the subscripts Na , K and M refer to sodium, potassium and M-type potassium channels respectively. A leak current is included with conductance g_L and reversal potential E_L , A is the membrane area, while I_{syn} is the current resulting from synaptic background activity. This model is capable of generating action potentials. Background activity in this case is modeled as a colored non-Gaussian noise, to take care of the

coupling due to the changes in the surrounding electric field that could affect the activity of the cell (ephaptic coupling), through a noise source with a certain temporal correlation.

We are interested in the initiation of the action potential, so we need only consider the sodium channels. Because the dynamics of potassium channels are too slow we can take them as unchanged. Moreover, near threshold given by $x_u \approx 10$ mV, the probability that a sodium channel is open depends only on the membrane voltage V . This probability is traditionally measured by the so-called activation curve, where $P_{Na}(V, t) = P_{Na}(V)$. Under these assumptions, Eq. (1) reduces to:

$$C_m \frac{dV}{dt} = -\bar{g}_{Na} P_{Na}(V)(V - E_{Na}) - (\bar{g}_K + \bar{g}_M)(V - E_K) - g_L(V - E_L) - \frac{1}{A} I_{syn}. \quad (2)$$

Action potential onset can occur when V reaches V^* , where V^* is an unstable equilibrium of Eq. (2) in the absence of noise. Below V^* the membrane potential relaxes to its resting potential, whereas above V^* an action potential can occur. To study the dynamics near onset, we therefore write $V = V^* + x$, and expand Eq. (2) to leading order in x , obtaining:

$$\begin{aligned} \frac{dx}{dt} &= ax + \eta(t), \\ a &= -\frac{1}{C_m} \left(\bar{g}_{Na} \frac{dP_{Na}(V^*)}{dV} (V^* - E_{Na}) + \bar{g}_{Na} P_{Na}(V^*) + (\bar{g}_K + \bar{g}_M + g_L) \right), \\ \eta(t) &= -\frac{1}{AC_m} I_{syn}(V^*). \end{aligned}$$

We fix that an action potential is fired when the membrane potential V reached the value $V^* + x_u$. Then the neuron fired when $x(T) = x_u$, with T the firing time [24]. With this consideration the model becomes equivalent to an Integrate-and-Fire model with a stochastic current [25].

With the assumptions made above, the parameter a (which is the onset rapidity) is independent of time. Then, if we consider a colored non-Gaussian noise as in Ref. [11], the problem to solve becomes:

$$\dot{x} = ax + \eta(t), \quad (3)$$

$$\dot{\eta} = -\frac{1}{\tau} \frac{dV_q(\eta)}{d\eta} + \frac{1}{\tau} \xi(t), \quad (4)$$

where $\xi(t)$ is a Gaussian white noise of zero mean and correlation $\langle \xi(t)\xi(t') \rangle = 2D\delta(t - t')$. $V_q(\eta)$ is given by

$$V_q(\eta) = \frac{D}{\tau(q-1)} \ln \left[1 + \frac{\tau}{D} (q-1) \frac{\eta^2}{2} \right].$$

Without enter in details this process η has, for $q \in (1, 3)$, a Tsallis-exponential type stationary distribution. For a detailed description of this process see Ref. [11].

We can make an approximation, valid for $|q-1| \ll 1$ [13]. The approach is made to modify Eq. (4):

$$\frac{1}{\tau} \frac{dV_q(\eta)}{d\eta} = \frac{\eta}{\tau} \left[1 + \frac{\tau(q-1)\eta^2}{2D} \right]^{-1} \approx \frac{\eta}{\tau} \left[1 + \frac{\tau(q-1)\langle \eta^2 \rangle}{2D} \right]^{-1} \equiv a(q, \tau)\eta, \quad (5)$$

given that $\langle \eta^2 \rangle = \frac{2D}{\tau(5-3q)}$. In this equation, $a(q, \tau) = \frac{5-3q}{\tau 2(2-q)}$. After performing this approximation, we must solve:

$$\dot{x} = ax + \eta(t), \quad (6)$$

$$\dot{\eta} = -a(q, \tau)\eta + \frac{1}{\tau} \xi(t). \quad (7)$$

This is a kind of “renormalized” Ornstein–Uhlenbeck (OU) process. Let us remark that the path-integral representation in the configuration space of the transition probability for a process driven by OU noise was previously derived in [23]. For $q = 1$ we recover the common OU process in agreement with Ref. [11].

2.2. Path integral approach

In the following we use the “unified color noise approximation”(UCNA) [14,15]. This is an adiabatic-like elimination procedure [23], which consists in setting equal to zero all the terms \ddot{x} and \dot{x}^n with $2 \leq n$. This result can be obtained in two ways: (a) applying a direct adiabatic-like elimination procedure to the Langevin system given by Eqs. (6) and (7). That is, taking the derivative of Eq. (6) with respect to t and setting $\ddot{x} = 0$. (b) A formal one, through the application of the path-integral formalism to the indicated non-Markovian Langevin equations, which is provided with a consistent Markovian approximation scheme. We follow the second alternative, because it has the advantage that we know exactly which terms of the dynamics are ignored [11,12]. The Fokker–Planck equation (FPE) associated to Eqs. (6) and (7) is:

$$\frac{\partial P_q}{\partial t} = -\frac{\partial}{\partial x} ((ax + \eta)P_q) + \frac{\partial}{\partial \eta} (a(q, \tau)\eta P_q) + \frac{D}{\tau^2} \frac{\partial^2 P_q}{\partial \eta^2}. \quad (8)$$

Since the diffusion matrix is singular, we can extend the number of variables (adding the canonically conjugate variables to $x(t)$ - $p_x(t)$ - and $\eta(t)$ - $p_\eta(t)$ -) and write the path-integral representation for the transition probability corresponding to the FPE:

$$P_q = \int_{x(0)=0, \eta=\eta_0}^{x(T)=x_u, \eta=\eta_u} \mathcal{D}[x(t)] \mathcal{D}[p_x(t)] \mathcal{D}[\eta(t)] \mathcal{D}[p_\eta(t)] e^{S_{q,1}}, \tag{9}$$

$S_{q,1}$ is the stochastic action given by:

$$S_{q,1} = \int_0^T ds \left(ip_x(s) [\dot{x}(s) - ax(s) - \eta(s)] + ip_\eta(s) \left[\dot{\eta}(s) + a(q, \tau)\eta + \frac{D}{\tau^2}(ip_\eta(s))^2 \right] \right). \tag{10}$$

The integration over $p_\eta(s)$ is Gaussian, yielding:

$$P_q = \int_{x(0)=0, \eta=\eta_0}^{x(T)=x_u, \eta=\eta_u} \mathcal{D}[x(t)] \mathcal{D}[\eta(t)] \mathcal{D}[p_x(t)] e^{S_{q,2}} \tag{11}$$

in which $S_{q,2}$ is:

$$S_{q,2} = \int_0^T ds \left(ip_x(s) [\dot{x}(s) - ax(s) - \eta(s)] + \frac{\tau^2}{4D} \int_0^T ds' [\dot{\eta}(s) + a(q, \tau)\eta(s)] \delta(s - s') [\dot{\eta}(s') + a(q, \tau)\eta(s')] \right). \tag{12}$$

The integration over $p_x(s)$ gives:

$$P_q = \int_{x(0)=0, \eta=\eta_0}^{x(T)=x_u, \eta=\eta_u} \mathcal{D}[x(t)] \mathcal{D}[\eta(t)] \hat{\delta}[\dot{x}(s) - ax(s) - \eta(s)] e^{S_{q,3}} \tag{13}$$

with

$$S_{q,3} = \int_0^T ds \frac{\tau^2}{4D} (\dot{\eta}(s) + a(q, \tau)\eta(s))^2, \tag{14}$$

and $\hat{\delta}[\dot{x}(s) - ax(s) - \eta(s)]$ means that, at each instant of time, we have

$$\eta(s) = \dot{x}(s) - ax(s). \tag{15}$$

The integration over $\eta(s)$ just corresponds to replacing $\eta(s)$ by $\dot{x}(s) - ax(s)$ and $\dot{\eta}(s)$ by $\ddot{x}(s) - a\dot{x}(s)$. The resulting stochastic action corresponds to a non-Markovian description as it involves $\ddot{x}(s)$. Doing the adiabatic elimination, which implies neglecting the term $\ddot{x}(s)$, we get:

$$\dot{\eta}(s) + a(q, \tau)\eta(s) \approx (a(q, \tau) - a)\dot{x}(s) - a(q, \tau)ax(s). \tag{16}$$

The final result for the transition probability is

$$P_q = \int_{x(0)=0, \eta=\eta_0}^{x(T)=x_u, \eta=\eta_u} \mathcal{D}[x(t)] e^S \tag{17}$$

with

$$S = \frac{1}{4D} \int_0^T ds \left(\frac{\dot{x}}{g} - \frac{f}{g}x \right)^2. \tag{18}$$

For sake of simplicity we write $f = a \frac{1}{1 - \frac{a}{a(q, \tau)}}$ and $g = \frac{1}{\tau a(q, \tau) (1 - \frac{a}{a(q, \tau)})}$.

Based on the previous assumptions, in the Results section we present the path integral solution of HH equation as the transition probability $P_q(x_u, T|0, 0)$, when considering a non-Gaussian colored noise q . Despite the formalism is derived using a pure analytical approach, it can be used to describe the emergent properties of the neuronal systems. It is important to point out that the result obtained is an approximated solution of the original problem specified in Eqs. (3) and (4). This is due to the followings approximations: one performed in Eq. (5), valid for $|q - 1| \ll 1$, and the other that corresponds to an adiabatic elimination realized in Eq. (16).

2.3. Information theory approach

We can define an Information Theory quantifier as a measure that is able to characterize some property of the probability distribution function associated with the time series of a given row signal (i.e. a neuron’s membrane potential). Entropy, regarded as a measure of uncertainty, is the most paradigmatic example of these quantifiers. Given a continuous transition probability $P_q(x_u, T|0, 0)$ or a given probability distribution function (PDF), and $\int_{\Delta} P_q(x_u, T|0, 0) dx_u = 1$, its associated Shannon Entropy S [26] is

$$S[P_q(x_u, T|0, 0)] = - \int_{\Delta} P_q(x_u, T|0, 0) \ln(P_q(x_u, T|0, 0)) dx_u. \tag{19}$$

Note that $P_q(x_u, T|0, 0)$ is characterized by a parameter q , which conveys departure from the pure Gaussian noise ($q = 1$).

In practice we consider $P_q(x_u, T|0, 0)$ of length N , that is $\mathcal{X}(t) \equiv \{x_t; t = 1, \dots, N\}$. Thus for a chosen discretization and the associated PDF, given by $P \equiv \{p_j; j = 1, \dots, N\}$ with $\sum_{j=1}^N p_j = 1$ and N the number of possible states of the system under study, the Shannon’s logarithmic information measure [26] is defined by (see Refs. [27–29])

$$S[P_q] = - \sum_{j=1}^N P_{q_j} \ln(P_{q_j}). \tag{20}$$

As $P_q(x_u, T|0, 0)$, which is the solution of the stochastic HH equation, accounts for the temporal causality (see Eq. (32)), this functional is equal to zero when we are able to predict with full certainty which of the possible outcomes j , whose probabilities are given by p_j , will actually take place. Our knowledge of the underlying process, described by the probability distribution, is maximal in this instance. In contrast, this knowledge is commonly minimal for a uniform distribution $P_e = \{p_j = 1/N, \forall j = 1, \dots, N\}$.

The Shannon entropy S is a measure of “global character” that is not too sensitive to strong changes in the PDF taking place in small region. Such is not the case with the Fisher information measure [30,31]

$$F[P_q] = \int \frac{|\vec{\nabla} P_q(x)|^2}{P_q(x)} dx, \tag{21}$$

which constitutes a measure of the gradient content of the distribution $P_q(x)$ (continuous PDF), thus being quite sensitive even to tiny localized perturbations.

The Fisher information measure can be variously interpreted as a measure of the ability to estimate a parameter, as the amount of information that can be extracted from a set of measurements, and also as a measure of the state of disorder of a system or phenomenon [31,32], its most important property being the so-called Cramer–Rao bound. It is important to remark that the gradient operator significantly influences the contribution of minute local P_q -variations to the Fisher information value, so that the quantifier is called a “local” one. Note that Shannon entropy decreases with skewed distribution, while Fisher information increases in such a case. Local sensitivity is useful in scenarios whose description necessitates an appeal to a notion of “order” [33–35]. The concomitant problem of loss of information due to the discretization has been thoroughly studied (see, for instance, Refs. [36–38] and references therein) and, in particular, it entails the loss of Fisher’s shift-invariance, which is of no importance for our current work. Phenomena, such as Poisson processes, do not obey shift invariance. Importantly the discrete version of Fisher information we present below is also valid when there is no shift invariance [39].

For Fisher information measure computation (discrete PDF) we follow the proposal of Dehesa and coworkers [40] based on amplitude of probability $P_q(x) = \psi(x)^2$ then

$$F[\psi] = 4 \int \left\{ \frac{d\psi}{dx} \right\}^2 dx. \tag{22}$$

Its discrete normalized version ($0 \leq F \leq 1$) is now

$$F[P_q] = F_0 \sum_{i=1}^{N-1} (\sqrt{P_{q_{i+1}}} - \sqrt{P_{q_i}})^2. \tag{23}$$

Here the normalization constant F_0 reads

$$F_0 = \begin{cases} 1 & \text{if } P_{q_{i^*}} = 1 \text{ for } i^* = 1 \text{ or } i^* = N \text{ and } P_{q_i} = 0 \forall i \neq i^* \\ 1/2 & \text{otherwise.} \end{cases} \tag{24}$$

Consequently, in the definition given by Eq. (22), the indicated integral becomes a weighted sum. This definition is also valid in the case of no shift-invariance as stated in Ref. [39]. If our system is in a very ordered state and thus is represented by a very narrow PDF, we have a Shannon entropy $S \sim 0$ and a Fisher information measure $F \sim F_{max}$. On the other hand, when the system under study lies in a very disordered state one gets an almost flat PDF and $S \sim S_{max}$, while $F \sim 0$. Of course, S_{max} and F_{max} are, respectively, the maximum values for the Shannon entropy and Fisher information measure. One can state that the general behavior of the Fisher information measure is opposite to that of the Shannon entropy [41].

In the following we consider the MPR statistical complexity [42] as it is able quantify critical details of dynamical processes underlying the data set. Based on the seminal notion advanced by López-Ruiz et al. [43], this statistical complexity measure is defined through the product

$$C_{JS}[P_q] = \mathcal{Q}_J[P_q, P_e] \cdot H[P_q] \tag{25}$$

of the normalized Shannon entropy

$$H[P_q] = S[P_q]/S_{max} \tag{26}$$

with $S_{max} = S[P_e] = \ln N$, ($0 \leq H \leq 1$) and the disequilibrium \mathcal{Q}_j defined in terms of the Jensen–Shannon divergence. That is,

$$\mathcal{Q}_j[P_q, P_e] = \mathcal{Q}_0 \mathcal{J}[P_q, P_e] \tag{27}$$

with

$$\mathcal{J}[P_q, P_e] = S[(P_q + P_e)/2] - S[P_q]/2 - S[P_e]/2 \tag{28}$$

the above-mentioned Jensen–Shannon divergence and \mathcal{Q}_0 , a normalization constant ($0 \leq \mathcal{Q}_j \leq 1$), are equal to the inverse of the maximum possible value of $\mathcal{J}[P_q, P_e]$. This value is obtained when one of the components of P_q , say p_m , is equal to one and the remaining p_j are equal to zero. The Jensen–Shannon divergence, which quantifies the difference between two (or more) probability distributions, is especially useful to compare the symbolic composition between different sequences [44]. Note that the above introduced statistical complexity measure (SCM) depends on two different probability distributions, the one associated with the system under analysis, P_q , and the uniform distribution, P_e .

3. Results

Let us remark that we have performed an approximation, valid for $|q - 1| \ll 1$ as in Ref. [13] in order to modify Eq. (4). Following Ref. [12] one can provide the exact solution of the path integral presented in Eq. (17), and the result for the transition probability $P_q(x_u, T|0, 0)$ reads as:

$$P_q(x_u, T|0, 0) = \left[2\pi D \left(\frac{\partial x_r(T)}{\partial \dot{x}_r(0)} \right) \right]^{-1/2} \exp(S[x_r(t)]), \tag{29}$$

where $x_r(t)$ is a reference path (typically the most likely trajectory, or “classical”, one which minimizes the action $\delta S[x_r(t)] = 0$). These solutions take into account the probability for the most likely path and the Gaussian deviations around it. Let us emphasize again that the results showed in Eqs. (17), (18) and (29) are approximate solutions of the original problem specified in Eqs. (3) and (4). More specifically, we have performed an approximation of the non-Gaussian colored noise q , which is valid for $|q - 1| \ll 1$ [13], and we have carried out an “Effective Markovian Approximation” as in Ref. [11]. Thus, the solution obtained from the path integral is an approximate solution of the original problem depicted in Eqs. (3) and (4).

The associated Lagrangian for this problem is:

$$L[x, \dot{x}, t] = \frac{1}{4Dg^2} (\dot{x} - f x)^2, \tag{30}$$

so the “classical” solution with the boundary conditions $x(0) = 0$ and $x(T) = x_u$ is:

$$x_c(t) = x_u \frac{\sinh(ft)}{\sinh(fT)}. \tag{31}$$

Replacing this in Eq. (29) we obtain:

$$P_q(x_u, T|0, 0) = \left[\frac{2\pi D}{f} \sinh(fT) \right]^{-1/2} \exp \left[\frac{e^{-2fT} - 1}{8Df} \left(\frac{x_u f}{g \sinh(fT)} \right)^2 \right]. \tag{32}$$

Importantly, in the limit $q \rightarrow 1$ and $\tau \rightarrow 0$, we get $f \rightarrow a$ and $g \rightarrow 1$. We recover, in this case, the result obtained by Colwell et al. [24] for the Gaussian approach:

$$P_1(x_u, T|0, 0) = \left[\frac{2\pi D}{a} \sinh(aT) \right]^{-1/2} \exp \left[\frac{e^{-2aT} - 1}{8Da} \left(\frac{x_u a}{\sinh(aT)} \right)^2 \right]. \tag{33}$$

In the following we use the first passage time problem to obtain some relevant quantities [12]. Let us consider trajectories $x(t)$ subject to the boundary conditions $x(0) = 0$ and $x(T) = x_u$, where T is the time at which the voltage threshold is attained. There is a distribution of times T at which the threshold condition can be met. Moreover, for a given T , there is a distribution of voltages $x(T)$ that the trajectory might attain at time T . This distribution is characterized by a mean $x_*(T)$, as well as a variance $\delta x(T)^2$. The total variance of the voltage threshold is therefore given by

$$S_v^2 = \int P(T)x(T)^2 dT - \left(\int P(T)x(T) dT \right)^2 + \int P(T)E[\delta x(T)^2] dT \tag{34}$$

where $P(T)$ is the probability that the voltage threshold occurs at time T , and $E[\cdot]$ denotes the expectation. The first two terms of Eq. (34) make up the variance of mean values $x_*(T)$ that occur owing to the range of times T at which the threshold condition is met. The onset span S_v measures the variability of the voltage threshold for action potential initiation [24]. For each such time T , the final term sums the variance of voltages $x(T)$ likely to be reached about the mean value $x_*(T)$. Eq. (34) directly relates the onset span S_v to the diffusion coefficient D , the voltage threshold x_u , and the onset rapidity a .

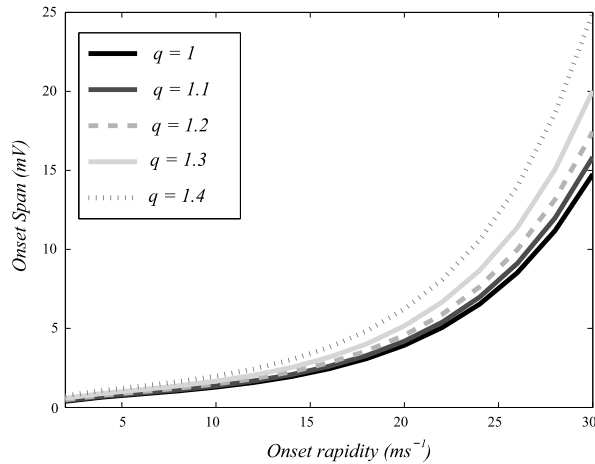


Fig. 1. Onset Span, S_v , versus the onset rapidity, a , for $\tau = 0.0015$, a diffusion coefficient $D = 25$ and $q = 1, 1.1, 1.2, 1.3$ and 1.4 , respectively.

Since in our model the threshold is fixed in the value x_u , the two first terms are zero, because the mean values $x_s(T)$ are all equals to the threshold x_u , and it is only the last term that survives, so the onset span is rising with the onset rapidity (parameter a in our model). The calculation of the last term in Eq. (34) is similar to the one performed in Ref. [24], and for our current model reads as:

$$E[\delta x(T)^2] = \frac{2Df^2}{T \tau a^2 a(q, \tau)^2} \sum_{n=0}^{\infty} \frac{1}{\frac{\pi^2}{T^2} (n + \frac{1}{2})^2 + f^2}. \tag{35}$$

The plot of the onset span as function of the onset rapidity a can be seen in Fig. 1, for a diffusion coefficient $D = 25$, correlation time $\tau = 0.0015$, and considering $q = 1, 1.1, 1.2, 1.3, 1.4$. Fig. 1 displays that the onset span increases as the level of noise q becomes higher. Also shows an intriguing relationship between variability of the onset potential at which an action potential occurs (the onset span) and the noise correlation q .

Fig. 2 shows the unnormalized transition probabilities P_q provided by Eq. (32), considering five values of $q = 1, 1.1, 1.2, 1.3$ and 1.4 . Note that as the values of q increases the distribution becomes sharper. In the following we illustrate how to use the path integral methodology, once obtained the transition probability associated to the Fokker–Planck equation as in Eq. (32), in order to characterize the dynamics of the spiking neural activity when considering a colored noise q . This could allow us to account for the possible effects of the surrounding background activity and the ephaptic coupling across the neuronal membrane. Indeed the application of nonlinear time series analysis provides us additional information, in comparison to the linear techniques, with useful insights about the correlational structure of the signal. More specifically, in the following we use subtle measures accounting for the nonlinear dynamic effects of the temporal signal: Shannon entropy [45,46] and the Martín–Plastino–Rosso (MPR) statistical complexity [45,46] within the entropy–complexity causality plane [47].

By estimating the statistical complexity versus the Shannon entropy [35,45–49], we show that it is possible to estimate the evolution of system trajectory to its maximum complexity path for a given amount of noise q . Fig. 3(a), (b), and (c) show the normalized Shannon entropy, the Fisher information and the statistical complexity versus q , respectively. In all the previous cases the normalized Shannon entropy, the Fisher information and the statistical complexity grows as the degree of noise q increases.

Let us recall that the maximum and minimum possible values of the generalized statistical complexity depends on the values of q [50,51]. Fig. 4(a) and (b) show that Fisher information grows as the entropy and statistical complexity becomes larger. Fig. 4(c) shows the informational causal plane of entropy versus complexity, $H \times C$. Note that the MPR statistical complexity grows linearly as the Shannon entropy becomes higher as the degree of noise q grows. Fig. 4(c) displays the maximum and minimum possible values of the generalized statistical complexity (continuous lines for different q). Note that the minimum and maximum value of the statistical complexity are reached at $q = 1$ and $q = 1.4$, respectively.

In contrast Fig. 5(a), (b), and (c) show the normalized Shannon entropy, the Fisher information and the statistical complexity versus q respectively, when considering a different diffusion coefficient D and onset rapidity a . In this case we present another scenario in which an optimal amount of noise correlation (controlled by q) leads to a maximum of the statistical complexity. Fig. 5(a) shows that the maximum entropy is reached when $q = 1.17$. Fig. 6(b) shows that Fisher information grows as q becomes larger. Fig. 5(c) shows that the statistical complexity is maximized when $q = 1.27$. The degree of order decreases as entropy increases, and thus a system with a lower degree of entropy is characterized by a higher degree of order. Fig. 6(a) shows Fisher information versus entropy, i.e., the causal information plane $F \times H$. Fig. 6(b) shows Fisher information versus the statistical complexity, i.e., the causal information plane $F \times C$, for the same diffusion

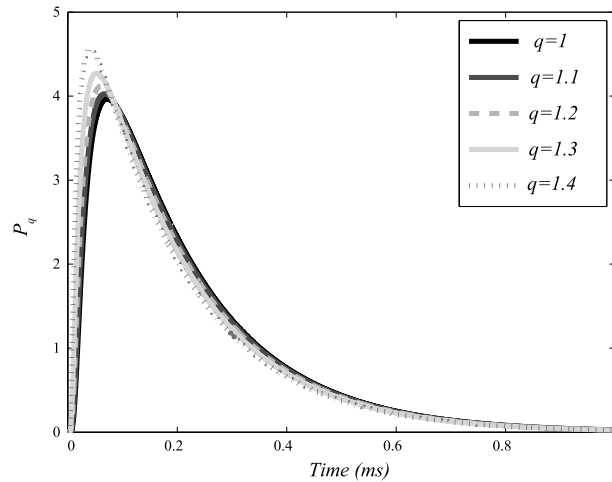


Fig. 2. Unnormalized transition probability, P_q , versus time (T). The diffusion coefficient is $D = 25$. The black curve correspond to the Gaussian noise $q = 1$; solid dark gray curve, $q = 1.1$; solid light gray curve, $q = 1.2$; dashed gray curve, $q = 1.3$; dotted gray curve, $q = 1.4$ (non-Gaussian noise).

coefficient D and onset rapidity a used above in Fig. 5(a), (b), and (c). Fig. 6(a) and (b) depict that Fisher information grows as the amount of noise q increases. So the system is in a very ordered state and thus is represented by a very narrow probability distribution, then we have a Shannon entropy close to zero and a maximal Fisher information measure as shown in Fig. 6(a). On the other hand when the system is in a very disordered state one gets an almost flat probability distribution and the entropy is maximal, while the Fisher information is smaller as shown in Fig. 6(a). The location of the maximum in the $H \times C$ causality plane allows us to infer useful information about the underlying dynamics of the path integral solution when considering the neural dynamics time series. Fig. 6(c) depicts $H \times C$, which shows that the maximum of the complexity is reached when the amount of noise q is optimal and equal to 1.27.

For the sake of completeness we show that taking different diffusion coefficients D and level of noise q it is possible to reproduce some of the prominent dynamical features of biological neurons as in Ref. [20]. Fig. 7 shows that we are able to reproduce the characteristics of the 20 different rhythmic activities as in Ref. [20], which includes also considering different input current (stimuli) proposed by Izhikevich [2], just by choosing different diffusion coefficients D and different level of noise q . The continuous lines represent the curves of maximum and minimum statistical complexity, C_{max} and C_{min} , respectively, as functions of the normalized Shannon entropy [20,50]. Note, however that as we are considering a correlated noise the neurons are not able to shoot with a fixed period as in Refs. [2,20]. Thus bursts are not therefore very likely to appear in this case when considering the different dynamics.

In this paper we use the methodology of path integrals, developed by Wio et al. considering a colored noise within the q -Gaussian formalism [11–13], to investigate the solutions of HH equation driven by a non-Gaussian colored noise q . We have shown that the complexity of the neuronal can be characterized by estimating the intrinsic correlational structure of the signal, modulated by q , considering the path integral solution of the HH stochastic equation. Fisher information increases as the amount of noise q becomes higher. Importantly, the causal entropy–complexity plane $H \times C$ allows us to identify and quantify the growing correlational structure of the neuronal dynamics. We have shown how the statistical complexity grows in the $H \times C$ plane reaching a maximum provided either by the optimal amount of noise or by the maximum/minimum possible value for the information measures that depend upon q [50,51]. This suggests the HH path integral solutions display a critical level of complexity for an optimal level of noise correlation q .

4. Discussion and conclusions

Developing theoretical tools that could provide new insights to study how mind/brain mechanisms behave can crucially change our understanding of cognitive processes. In this paper, we show that recent advances in complex systems can provide crucial new insights into this problem. Complexity captures the degree to which a neural system integrates specialized information, and in particular, the complexity of the neural system represent the amount of information contained in the organism, in the sense that it quantifies the dynamical features of the temporal pattern due to functional interactions produced by a structural network. Complexity captures the degree to which a neural system integrates specialized information, and in particular, MPR statistical complexity can distinguish time series generated by stochastic and chaotic systems [45,46]. This statistical complexity measure can also detect and quantify noise induced order [45,46].

In this paper we present a novel theoretical approach to investigate the path integral solutions of HH equation driven by a colored noise q . More specifically we provide the analytical solution driven by a non-Gaussian colored noise when considering the stochastic versions of the HH equations, taking into account subtle processes that could be induced by

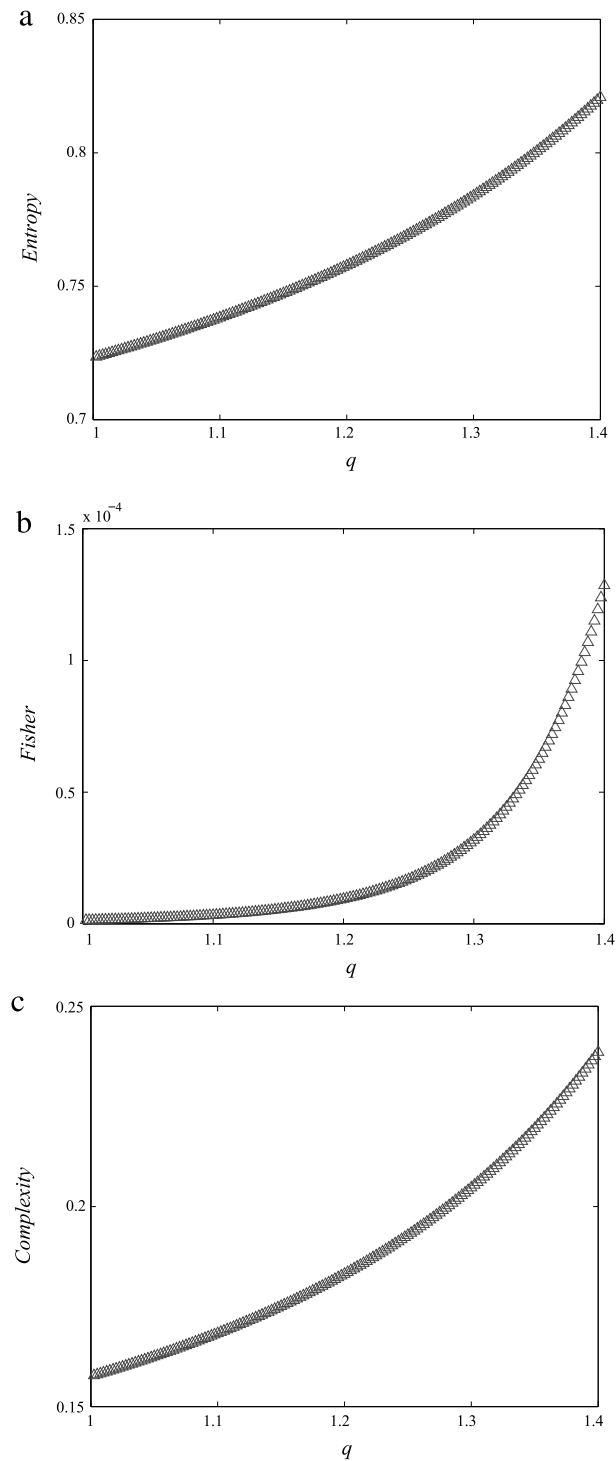


Fig. 3. The information quantifiers versus q considering a diffusion coefficient $D = 4$ and an onset rapidity $a = 0.211 \text{ m s}^{-1}$. (a) Causal Fisher information versus q . (b) Causal Fisher information versus q . (c) Statistical complexity versus q .

the surrounding neural network and by feedforward correlations. Importantly, we recover the results obtained within the Gaussian approach, for the stochastic HH equations [24], in the limit $q \rightarrow 1$ and $\tau \rightarrow 0$. We investigate then the causality entropy–complexity plane $H \times C$ and Fisher information versus MPR statistical complexity/Shannon entropy considering the solution of the path integral formulation driven by different levels of noise q . This permits characterizing

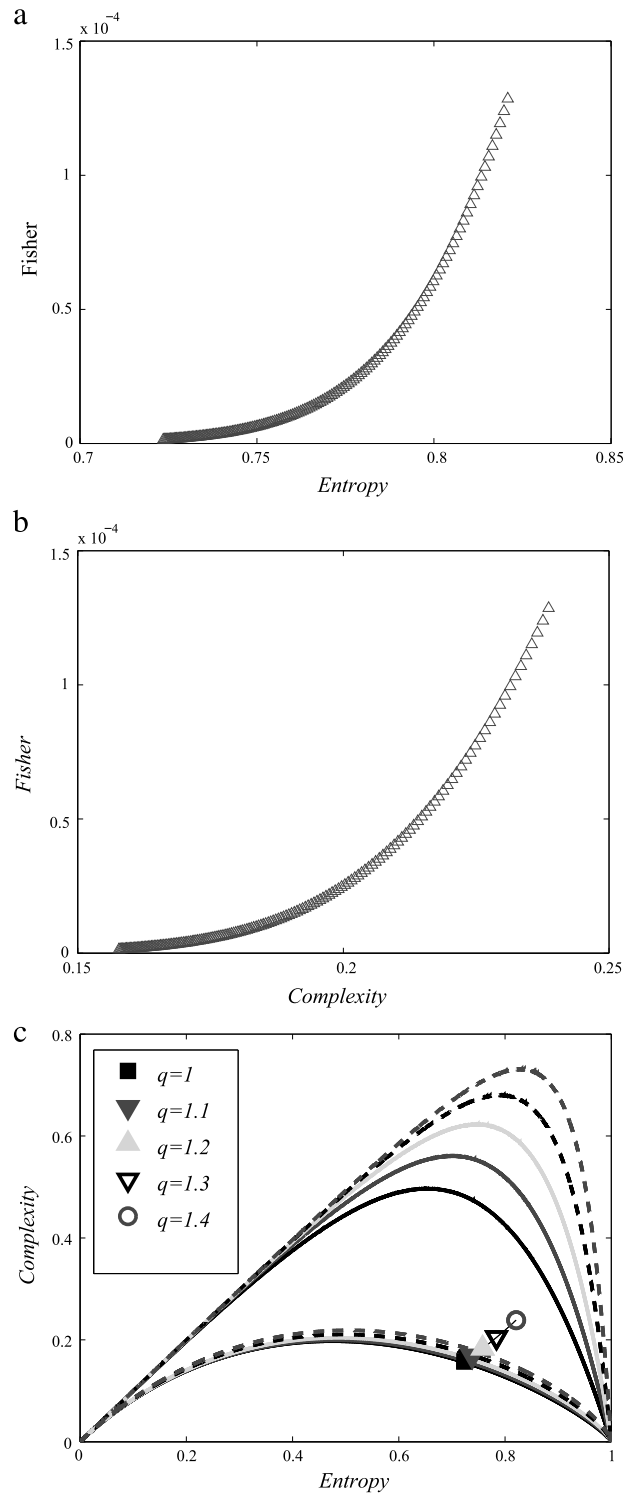


Fig. 4. The informational causal plane considering a diffusion coefficient $D = 4$, an onset rapidity $a = 0.211 \text{ m s}^{-1}$ and that q can change freely. (a) Causal Fisher information versus normalized Shannon entropy ($F \times H$ plane). (b) Causal Fisher information versus statistical complexity ($F \times C$ plane). (c) Statistical complexity versus normalized Shannon Entropy ($C \times H$ plane). The upper and lower curves are the maximum, and minimum complexity, respectively for different q values. Solid black curve, $q = 1$; solid dark gray curve, $q = 1.1$; solid light gray curve, $q = 1.2$; dashed black curve, $q = 1.3$; dashed dark gray curve, $q = 1.4$.

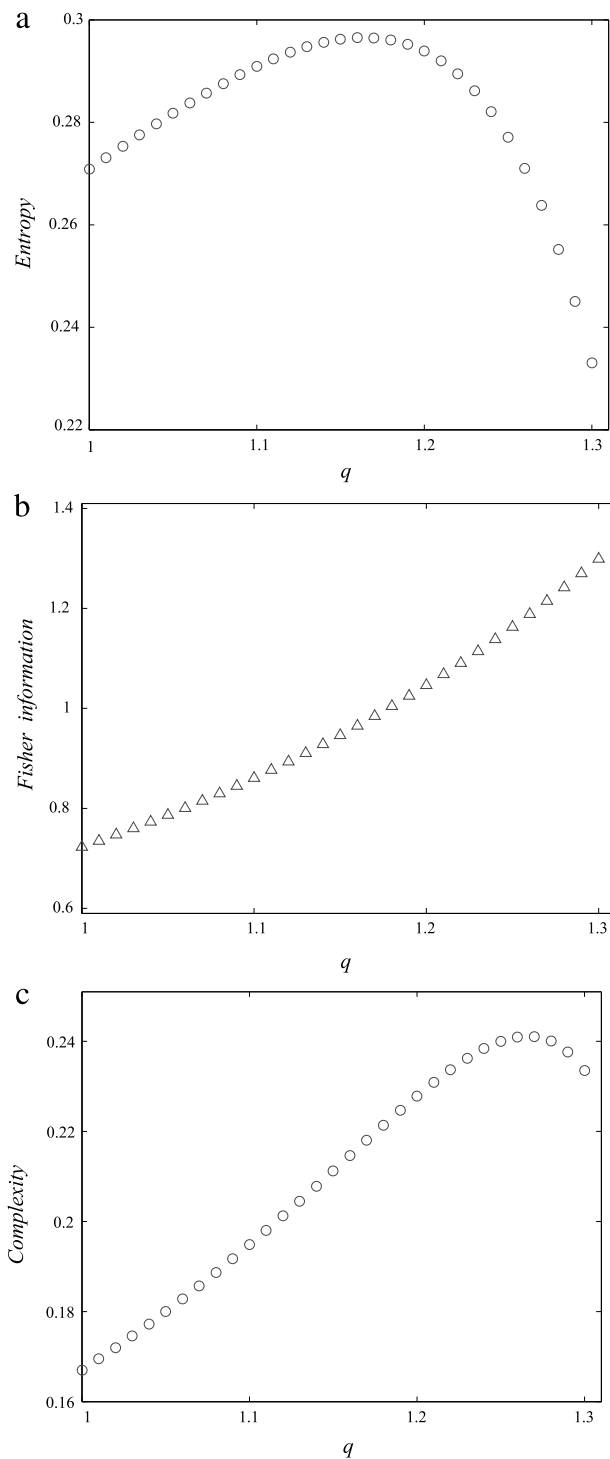


Fig. 5. The information quantifiers versus q considering that the onset rapidity is $a = 26.33 \text{ m s}^{-1}$. The diffusion coefficient D takes values between 1.63 and 1.71, and that q can change freely. (a) Causal Fisher information versus q . (b) Causal Fisher information versus q . (c) Statistical complexity versus q .

the internal dynamics of the neuron when taking into account different degrees of noise. We show that the maximum of the complexity is reached when the amount of noise q is optimal. Importantly, we show that using the path integral solution in combination with complexity measures our results resemble the prominent dynamical features of biological neurons as in Ref. [20]. Moreover, the current model could be easily generalized by adding another variable accounting for the ionic

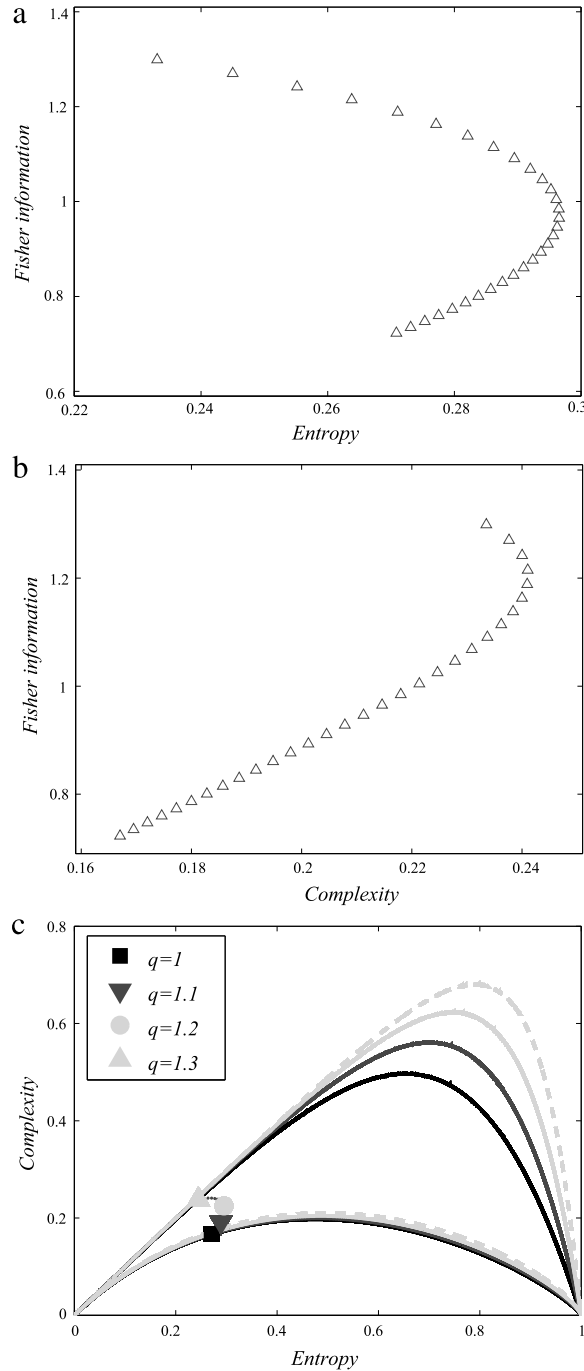


Fig. 6. The information quantifiers considering an onset rapidity $a = 26.33 \text{ m s}^{-1}$. The diffusion coefficient D takes values between 1.63 and 1.71, and that q can change freely. (a) Causal Fisher information versus q . (b) Causal Fisher information versus q . (c) Statistical complexity versus normalized Shannon Entropy ($C \times H$ plane). The upper and lower curves are the maximum, and minimum complexity, respectively for different q values. Black curve, $q = 1$; dark gray curve, $q = 1.1$; light gray curve, $q = 1.2$; dashed light gray curve, $q = 1.3$.

channels dependence to the stochastic equations. Despite the formalism presented in this paper has been derived using a pure analytical approach, it can be used in future research to compare experimental observations with the parameter values incorporated into such model.

Our approach allows us to characterize the dynamics of a Fokker–Planck neuron, quantifying the causality of the signal, and inferring the emergent properties of the system as the amount of noise q increases. The causal information plane

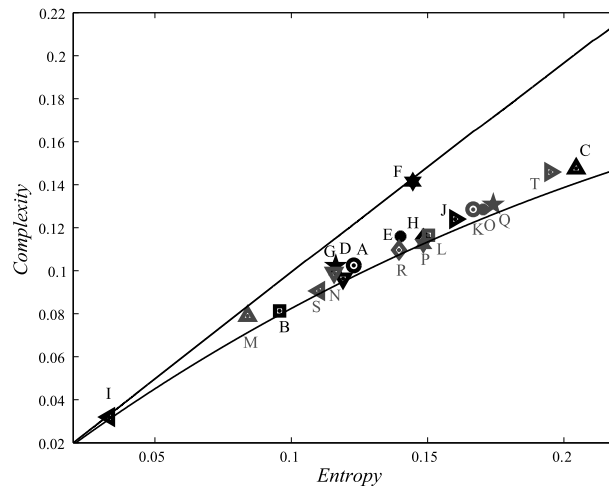


Fig. 7. Causal MPR complexity versus normalized Shannon entropy ($H \times C$ -plane) for the 20 most relevant neurocomputational features of biological neurons. Different diffusion coefficients D and level of noise q are considered. (A) $q = 1.15152$, $D = 4.22755$; (B) $q = 1.16268$, $D = 3.81318$; (C) $q = 1.12925$, $D = 6.89292$; (D) $q = 1.16062$, $D = 4.37179$; (E) $q = 1.13131$, $D = 5.16442$; (F) $q = 1.06566$, $D = 11.2422$; (G) $q = 1.10606$, $DD = 5.93473$; (H) $q = 1.17204$, $D = 3.78157$; (I) $q = 1.10929$, $D = 0.0596582$; (J) $q = 1.13333$, $D = 6.21699$; (K) $q = 1.13373$, $D = 6.0347$; (L) $q = 1.14465$, $D = 5.71361$; (M) $q = 1.15476$, $D = 2.73747$; (N) $q = 1.11594$, $D = 6.09513$; (O) $q = 1.14815$, $D = 5.45674$; (P) $q = 1.17733$, $D = 3.86789$; (Q) $q = 1.14103$, $D = 5.99206$; (R) $q = 1.14815$, $D = 5.45674$; (S) $q = 1.16667$, $D = 3.87343$; (T) $q = 1.13333$, $D = 5.77569$.

can be profitably used to separate and differentiate amongst chaotic and deterministic systems [33,52]; visualization and characterization of different dynamical regimes when the system parameters vary [33–35]; time dynamic evolution [53]; identifying periodicities in natural time series [54]; identification of deterministic dynamics contaminated with noise [55,56] and estimating intrinsic time scales of delayed systems [47,57,58]; among other applications [48].

According to the theorem of Liouville in the case of dissipative systems (non-energy preserving), the volume occupied by the states in the phase space shrinks as time goes towards infinity. The limit set of an autonomous dissipative system to which trajectories converge for time increasing towards infinity is called the attractor. As the noise correlation q grows, the dendrites of the neuron dissipate large quantities of their metabolic energy. The dissipation in this case manifests itself in the disappearance of energy and the emergence of a complex network structure. In this paper, we show that the different path of the solution for different levels of noise q can be associated with a complex dynamic reflected in the causality entropy–complexity plane, $H \times C$. The effects of the network inter-connectivity and the possible ephaptic coupling of given neuron is summarized through the parameter q , which may be essential for integrating the actions of individual neurons and therefore for enabling cognitive processes such as perception, attention, and memory. We are currently working on a Metropolis simulation that will allow us to further test the goodness of the results presented in this paper not just by contrasting them with the neuronal rhythm proposed by Izhikevich [2,20] as we showed here, but instead also using real neurophysiological data. Thus, using the path integral solution of the HH equations driven by a colored noise q in combination with the normalized Shannon entropy, Fisher information and statistical complexity, can help us to understand the subtle processes of the neural dynamics considering stochastic models, and information theory.

Acknowledgments

We gratefully acknowledge funding from PIP 11220130100327CO (2014/2016) CONICET, Argentina (F.M.) and Universidad Nacional de La Plata, Argentina (project 11/X716).

References

- [1] E.M. Izhikevich, Simple model of spiking neurons, *IEEE Trans. Neural Netw.* 14 (2003) 1569–1572.
- [2] E.M. Izhikevich, Which model to use for cortical spiking neurons?, *IEEE Trans. Neural Netw.* 15 (2004) 1063–1070.
- [3] E.M. Izhikevich, *Dynamical Systems in Neuroscience: The Geometry of Excitability and Bursting*, The MIT Press, Cambridge, Massachusetts, USA, 2007.
- [4] E.M. Izhikevich, Polychronization: computation with spikes, *Neural Comput.* 18 (2006) 245–282.
- [5] D. Johnston, S.M.S. Wu, *Foundations of Cellular Neurophysiology*, MIT Press, Cambridge, 1995.
- [6] L. Graham, Modelling neuronal biophysics, in: M. Arbib (Ed.), *The Handbook for Brain Theory and Neural Networks*, second ed, MIT Press, Cambridge, 2002, pp. 164–170.
- [7] P.S.G. Stein, S. Grillner, A.I. Selverston, D.G. Stuart (Eds.), *Neurons, Networks, and Motor Behavior*, MIT Press, Cambridge, 1997.
- [8] G. Laurent, M. Stopfer, R.W. Friedrich, M.I. Rabinovich, A. Volkovskii, H.D.I. Abarbanel, Odor encoding as an active dynamical process: experiments, computation, and theory, *Annu. Rev. Neurosci.* 24 (2001) 263–297.
- [9] C. Koch, *Biophysics of Computation: Information Processing in Single Neurons*, Oxford University Press, Oxford, 1999.
- [10] N. Brunel, Vincent Hakim, Sparsely synchronized neuronal oscillations, *Chaos* 18 (2008) 015113.

- [11] M.A. Fuentes, H.S. Wio, R. Toral, Effective markovian approximation for non-gaussian noises: a path integral approach, *Physica A* 303 (2002) 91–104.
- [12] H.S. Wio, *Path Integrals for Stochastic Processes - an Introduction*, World Scientific Publishing Company, 2013.
- [13] H.S. Wio, R. Toral, Effect of non-gaussian noise sources in a noise-induced transition, *Physica D* 103 (2004) 161–168.
- [14] P. Jung, P. Hänggi, Dynamical systems: a unified colored-noise approximation, *Phys. Rev. A* 35 (1987) 4464–4466.
- [15] P. Jung, P. Hänggi, Optical instabilities: new theories for colored-noise-driven laser instabilities, *J. Opt. Soc. Amer. B* 5 (1989) 979–986.
- [16] C.C. Chow, M.A. Buice, Path integral methods for stochastic differential equations, *J. Math. Neurosci.* 5 (2015) 8.
- [17] A.L. Hodgkin, A.F. Huxley, A quantitative description of membrane current and its application to conduction and excitation in nerve, *J. Neurophysiol.* 117 (1951) 500–544.
- [18] F. Montani, E.B. Deleglise, O.A. Rosso, Efficiency characterization of a large neuronal network: a causal information approach, *Physica A* 401 (2014) 58–70.
- [19] F. Montani, O.A. Rosso, F. Matias, S.L. Bressler, C.R. Mirasso, A symbolic information approach to determine anticipated and delayed synchronization in neuronal circuit models, *Philos. Trans. R. Soc. Lond. Ser. A* 373 (2015) 20150110.
- [20] F. Montani, R. Baravalle, L. Montangie, O.A. Rosso, Causal information quantification of prominent dynamical features of biological neurons, *Philos. Trans. R. Soc. Lond. Ser. A* 373 (2015) 20150109.
- [21] L. Montangie, F. Montani, Effect of interacting second- and third-order stimulus-dependent correlations on population-coding asymmetries, *Phys. Rev. E* 94 (2016) 042303.
- [22] C.A. Anastassiou, R. Perin, H. Markram, C. Koch, Ephaptic coupling of cortical neurons, *Nature Neurosci.* 14 (2011) 217–223.
- [23] H.S. Wio, P. Colet, M. San Miguel, L. Pesquera, M.A. Rodríguez, Path-integral formulation for stochastic processes driven by colored noise, *Phys. Rev. A* 40 (1989) 7312–7324.
- [24] L.J. Colwell, M.P. Brenner, Action potential initiation in the Hodgkin–Huxley model, *PLoS Comput. Biol.* 5 (1) (2009) e1000265.
- [25] P. Dayan, L.F. Abbott, *Theoretical Neuroscience: Computational and Mathematical Modeling of Neural Systems*, MIT press, 2001.
- [26] C. Shannon, W. Weaver, *The Mathematical Theory of Communication*, University of Illinois Press, Champaign, Illinois, USA, 1949.
- [27] F. Montani, E. Phoka, M. Portesi, S.R. Schultz, Statistical modelling of higher-order correlations in pools of neural activity, *Physica A* 392 (2013) 3066–3086.
- [28] L. Montangie, F. Montani, Quantifying higher-order correlations in a neuronal pool, *Physica A* 421 (2015) 388–400.
- [29] L. Montangie, F. Montani, Higher-order correlations in common input shapes the output spiking activity of a neural population, *Physica A* 471 (2017) 845–861.
- [30] R.A. Fisher, On the mathematical foundations of theoretical statistics, *Philos. Trans. R. Soc. Lond. Ser. A* 222 (1922) 309–368.
- [31] B. Roy Frieden, *Science from Fisher Information: A Unification*, Cambridge University Press, Cambridge, 2004.
- [32] A.L. Mayer, C.W. Pawlowski, H. Cabezas, Fisher information and dynamic regime changes in ecological systems, *Ecol. Modell.* 195 (2006) 72–82.
- [33] F. Olivares, A. Plastino, O.A. Rosso, Contrasting chaos with noise via local versus global information quantifiers, *Phys. Lett A* 376 (2012) 1577–1583.
- [34] O.A. Rosso, L. De Micco, A. Plastino, H.A. Larrondo, Info-quantifiers’ map-characterization revisited, *Physica A* 389 (2010) 249–262.
- [35] F. Olivares, A. Plastino, O.A. Rosso, Ambiguities in the Bandt-Pompe’s methodology for local entropic quantifiers, *Physica A* 391 (2012) 2518–2526.
- [36] K. Zografos, K. Ferentinos, T. Papaioannou, Discrete approximations to the Csiszár, Rényi, and Fisher measures of information, *Canad. J. Statist.* 14 (1986) 355–366.
- [37] L. Pardo, D. Morales, K. Ferentinos, K. Zografos, Discretization problems on generalized entropies and R-divergences, *Kybernetika* 30 (1994) 445–460.
- [38] M. Madiman, O. Johnson, I. Kontoyiannis, Fisher Information compound Poisson approximation, and the Poisson channel, in: *IEEE Int. Symp. Inform. Th. Nice, June 2007*.
- [39] R. Frieden, R.A. Gatenby, *Exploratory Data Analysis using Fisher Information Vol. 377*, Springer-Verlag, London, 2011, p. 377.
- [40] P. Sanchez-Moreno, J.S. Dehesa, R.J. Yanez, Discrete densities and fisher information, in: *Proceedings of the 14th International Conference on Difference Equations and Applications*, Uğur-Bahçeşehir University Publishing Company, Istanbul, Turkey, 2009, pp. 291–298 *Difference Equations and Applications*.
- [41] F. Pennini, A. Plastino, Reciprocity relations between ordinary temperature and the Frieden-Soffer Fisher temperature, *Phys. Rev. E* 71 (2005) 047102.
- [42] P.W. Lambert, M.T. Martín, A. Plastino, O.A. Rosso, Intensive entropic non-triviality measure, *Physica A* 334 (2004) 119–131.
- [43] R. López-Ruiz, H.L. Mancini, X. Calbet, A statistical measure of complexity, *Phys. Lett. A* 209 (1995) 321–326.
- [44] I. Grosse, P. Bernaola-Galván, P. Carpena, R. Román-Roldán, J. Oliver, H.E. Stanley, Analysis of symbolic sequences using the Jensen–Shannon divergence, *Phys. Rev. E* 65 (2002) 041905.
- [45] O.A. Rosso, C. Masoller, Detecting and quantifying stochastic and coherence resonances via information-theory complexity measurements, *Phys. Rev. E* 79 (2009) 040106(R).
- [46] O.A. Rosso, C. Masoller, Detecting and quantifying temporal correlations in stochastic resonance via information theory measures, *Eur. Phys. J. B* 69 (2009) 37–43.
- [47] L. Zunino, M.C. Soriano, O.A. Rosso, Distinguishing chaotic and stochastic dynamics from time series by using a multiscale symbolic approach, *Phys. Rev. E* 86 (2012) 046210.
- [48] M. Zanin, L. Zunino, O.A. Rosso, D. Papo, Permutation entropy and its main biomedical and econophysics applications: a review, *Entropy* 14 (2012) 1553–1577.
- [49] F. Montani, O.A. Rosso, Entropy-Complexity characterization of brain development in chickens, *Entropy* 16 (8) (2014) 4677–4692.
- [50] M.T. Martín, A. Plastino, O.A. Rosso, Generalized statistical complexity measures: geometrical and analytical properties, *Physica A* 369 (2006) 439–462.
- [51] O.A. Rosso, M.T. Martín, H.A. Larrondo, A.M. Kowalski, A. Plastino, *Generalized Statistical Complexity: A New Tool for Dynamical Systems*, Bentham Science Publishers, 2013, pp. 277–302.
- [52] O.A. Rosso, H.A. Larrondo, M.T. Martín, A. Plastino, M.A. Fuentes, Distinguishing noise from chaos, *Phys. Rev. Lett.* 99 (2007) 154102.
- [53] A. Kowalski, M.T. Martín, A. Plastino, O.A. Rosso, Bandt-Pompe approach to the classical-quantum transition, *Physica D* 233 (2007) 21–31.
- [54] C. Bandt, Ordinal time series analysis, *Ecol. Modell.* 182 (2005) 229–238.
- [55] O.A. Rosso, L.C. Carpi, P.M. Saco, M. Gómez Ravetti, A. Plastino, H.A. Larrondo, Causality and the entropy–complexity plane: robustness and missing ordinal patterns, *Physica A* 391 (2012) 42–55.
- [56] O.A. Rosso, L.C. Carpi, P.M. Saco, M. Gómez Ravetti, A. Plastino, H.A. Larrondo, The Amigó paradigm of forbidden/missing patterns: a detailed analysis, *Eur. Phys. J. B* 85 (2012) 419.
- [57] L. Zunino, M.C. Soriano, I. Fischer, O.A. Rosso, C.R. Mirasso, Permutation-information-theory approach to unveil delay dynamics from time-series analysis, *Phys. Rev. E* 82 (2010) 046212.
- [58] M.C. Soriano, L. Zunino, O.A. Rosso, I. Fischer, C.R. Mirasso, Time scales of a chaotic semiconductor laser with optical feedback under the lens of a permutation information analysis, *IEEE J. Quantum Electron.* 47 (2011) 252–261.